Accumulation and Erosion of Mars' South Polar Layered Deposits

Roberto Seu, *et al.*

Science **317**, 1715 (2007);
DOI: 10.1126/science.1144120

Science (print ISSN 0036-8075; online ISSN 1095-9203) is published weekly, except the last week in December, by the American Association for the Advancement of Science, 1200 New York Avenue NW, Washington, DC 20005.

beds" is suggestive of a repeating climate signal within the upper PLD.

These observations are consistent with the following general history of the north polar region. (i) Dark sand saltates into the north polar region during periods (possibly high obliquity) when thick accumulations of ice do not form at the north pole. (ii) Alternating with sand migration, ice accumulates and inhibits saltation of underlying dark sand (possibly during lower obliquity). (iii) Several such depositional cycles produce alternating brighter (ice and dust) and darker (sandy) layers in the basal unit. (iv) Icy layers, similar in morphology to those in the basal unit, are deposited with little or no dark sand to form the lower (polygonally cracked) PLD. This transition from the previous depositional cycles may indicate that the sand supply was exhausted or no longer transportable onto these growing deposits. (v) The upper PLD accumulates, and varying conditions during its accumulation lead to the development of the layered sequences that have been correlated in multiple exposures (*6*, *22*). (vi) Most recently, the thin north polar residual cap forms on top of the PLD and evolves to its present state by condensation and sublimation of water ice. Mass wasting of the PLD at steep scarps produces icy debris fans.

References and Notes

1. S. Byrne, B. Murray, *J. Geophys. Res.* **107**, 10.1029/2001JE001615 (2002).
2. K. Edgett, R. M. E. Williams, M. C. Malin, B. A. Cantor, P. C. Thomas, *Geomorphology* **52**, 289 (2003).
3. K. Fishbaugh, J. Head, *Icarus* **174**, 444 (2005).
4. P. Thomas, S. Squyres, K. Herkenhoff, A. Howard, B. Murray, in *Mars* (Univ. Arizona Press, Tucson, 1992).
5. Y. Langevin F. Poulet, J.-P. Bibring, B. Gondet, *Science* **307**, 1584 (2005); published online 17 February 2005 (10.1126/science.1109091).
6. K. Tanaka, *Nature* **437**, 991 (2005).
7. S. Clifford *et al.*, *Icarus* **174**, 291 (2005).
8. A. McEwen *et al.*, *J. Geophys. Res.* **112**, 10.1029/2005JE002605 (2007).
9. L_s is the solar longitude of Mars, used to define season with 0 defined as the northern vernal equinox.
10. R. J. Phillips et al., *Lunar Planet. Sci. Conf.* **XXXVIII**, abstr. 1925 (2007).
11. S. Murchie *et al.*, *Lunar Planet. Sci. Conf.* **XXXVIII**, abstr. 1472 (2007).
12. A. Johnson, *Physical Processes in Geology* (Freeman, New York, 1970).
13. R. Seu *et al.*, *Science* **317**, 1715 (2007).
14. M. Malin, K. Edgett, *J. Geophys. Res.* **106**, 23439 (2001).
15. S. Milkovich, J. Head, *J. Geophys. Res.* **110**, 10.1029/2004JE002349 (2005).
16. HiRISE images are identified by the format "mission phase_orbit number_orbital position." For example, PSP_001738_2670 was acquired in the Primary Science Phase, orbit 1738, and 267° from the night-side equator or 87°N latitude (MRO travels north over the day side in its orbit).
17. J. Cutts, B. Lewis, *Icarus* **50**, 216 (1982).
18. J. Laskar, B. Levrard, F. Mustard, *Nature* **419**, 375 (2002).
19. L. Fenton, K. Herkenhoff, *Icarus* **147**, 433 (2000).
20. A. Howard, J. Cutts, K. Blasius, *Icarus* **50**, 161 (1982).
21. E. Kolb, K. Tanaka, *Icarus* **154**, 22 (2001).
22. K. Fishbaugh, C. Hvidberg, *J. Geophys. Res.* **111**, 10.1029/2005JE002571 (2006).
23. S. M. Milkovich, J. W. Head III, *Mars* 2, 21 (2006).

24. We thank the HiRISE science team and operations staff at the University of Arizona for continuing support in acquiring spectacular images of the martian polar regions and the USGS HiRISE team for development of software and procedures for processing the images. Two anonymous reviews and comments by J. Skinner and K. Tanaka helped to improve the manuscript and are much appreciated.

6 April 2007; accepted 28 August 2007
10.1126/science.1143544

REPORT

Accumulation and Erosion of Mars' South Polar Layered Deposits

Roberto Seu,[1]* Roger J. Phillips,[2] Giovanni Alberti,[3] Daniela Biccari,[1] Francesco Bonaventura,[4] Marco Bortone,[3] Diego Calabrese,[5] Bruce A. Campbell,[6] Marco Cartacci,[1] Lynn M. Carter,[6] Claudio Catallo,[5] Anna Croce,[5] Renato Croci,[5] Marco Cutigni,[1] Antonio Di Placido,[4] Salvatore Dinardo,[3] Costanzo Federico,[7] Enrico Flamini,[8] Franco Fois,[5] Alessandro Frigeri,[7] Oreste Fuga,[1] Emanuele Giacomoni,[1] Yonggyu Gim,[9] Mauro Guelfi,[5] John W. Holt,[10] Wlodek Kofman,[11] Carlton J. Leuschen,[12] Lucia Marinangeli,[13] Paolo Marras,[4] Arturo Masdea,[1] Stefania Mattei,[3] Riccardo Mecozzi,[5] Sarah M. Milkovich,[9] Antonio Morlupi,[4] Jérémie Mouginot,[11] Roberto Orosei,[14] Claudio Papa,[3] Tobia Paternò,[4] Paolo Persi del Marmo,[1] Elena Pettinelli,[15] Giulia Pica,[3] Giovanni Picardi,[1] Jeffrey J. Plaut,[9] Marco Provenziani,[1] Nathaniel E. Putzig,[2] Federica Russo,[1] Ali Safaeinili,[9] Giuseppe Salzillo,[3] Maria Rosaria Santovito,[3] Suzanne E. Smrekar,[9] Barbara Tattarletti,[4] Danilo Vicari[4]

Mars' polar regions are covered with ice-rich layered deposits that potentially contain a record of climate variations. The sounding radar SHARAD on the Mars Reconnaissance Orbiter mapped detailed subsurface stratigraphy in the Promethei Lingula region of the south polar plateau, Planum Australe. Radar reflections interpreted as layers are correlated across adjacent orbits and are continuous for up to 150 kilometers along spacecraft orbital tracks. The reflectors are often separated into discrete reflector sequences, and strong echoes are seen as deep as 1 kilometer. In some cases, the sequences are dipping with respect to each other, suggesting an interdepositional period of erosion. In Australe Sulci, layers are exhumed, indicating recent erosion.

A marked similarity between Mars and Earth is the presence of thick polar ice caps, which potentially provide a wealth of data about recent climate and atmospheric history (*1*, *2*). The martian polar plateaus are as much as 3.5 km thick (*3*) and composed of layers overlain by a residual (i.e., perennial) ice cap that, according to recent analyses, is no more than a few tens of meters thick (*4*–*6*). The polar residual ice in the south is predominantly CO_2 ice containing trace amounts of dust and water ice (*5*). Compared to the north, the residual ice covers only a small portion of the south polar layered deposits (SPLD), which are offset from the pole by ~2° and are asymmetrically distributed between latitudes 70°S and 80°S (*3*). Most plateau surfaces are buried under an optically thick layer of sand or of seasonal frost accumulations (*7*). The layers are composed of water ice mixed with dust, with layer thicknesses and ice/dust ratios possibly controlled by orbital cycles (*8*). They apparently formed by deposition of ice condensates or precipitates and atmospheric dust (*9*, *10*). The polar plateaus are considered to be very young. On the basis of crater counts, the surface age of Planum Australe is estimated to be on the order of tens of millions of years (*11*, *12*).

Planum Australe was probed previously with the Mars Advanced Radar for Subsurface and Ionospheric Sounding (MARSIS) onboard the European Space Agency's Mars Express (*6*, *13*). The MARSIS radar signals penetrated to depths estimated to be greater than 3.7 km (*6*). Subsurface echoes are frequently very strong, indicating minimal attenuation of the signal through

[1]Dipartimento INFOCOM, Università di Roma "La Sapienza," I-00184 Rome, Italy. [2]Washington University, St. Louis, MO 63130, USA. [3]Consorzio di Ricerca Sistemi di Telesensori Avanzati, I-80125 Naples, Italy. [4]Info Solution Spa, I-00131 Rome, Italy. [5]Thales Alenia Space Italia, I-00131 Rome, Italy. [6]Smithsonian Institution, Washington, DC 20013–7012, USA. [7]Università di Perugia, I-06123 Perugia, Italy. [8]Agenzia Spaziale Italiana, I-00198 Rome, Italy. [9]Jet Propulsion Laboratory, California Institute of Technology, Pasadena, CA 91109, USA. [10]University of Texas at Austin, Austin, TX 78758, USA. [11]CNRS and Université Joseph Fourier, 38041 Grenoble Cedex 9, France. [12]University of Kansas, Lawrence, KS 66045–7612, USA. [13]International Research School of Planetary Sciences, I-65127 Pescara, Italy. [14]Istituto Nazionale di Astrofisica, I-00133 Rome, Italy. [15]Università Roma Tre, I-00146 Rome, Italy.

*To whom correspondence should be addressed. E-mail: roberto.seu@uniroma1.it

the SPLD. Although plausible solutions to models of layer composition based on the dielectric losses are unconstrained (*14*), the SPLD may be composed of nearly pure water ice (*6*). With a vertical resolution of 150 m in free space, however, MARSIS is not suited to study the structure of the deposits, because individual layers are a few meters thick (*15*).

SHARAD (Shallow Radar) is a synthetic-aperture, orbital sounding radar on the Mars Reconnaissance Orbiter (MRO) (*16*). SHARAD was designed to complement MARSIS by trading penetration depth for improved vertical resolution (*17*, *18*) and is better suited for mapping 10-m-scale stratigraphy in the polar plateaus. Data are collected preferentially on the night side of Mars, where the Sun-excited ionosphere has a low electron density and plasma frequency, and radar echoes are thus nearly unaffected by distortions caused by propagation through a frequency-dispersive medium. SHARAD operates at a center frequency of 20 MHz, with a 10-MHz bandwidth that provides a free-space range resolution of ~15 m after pulse compression. Resolution in the across-track direction ranges from 3 to 6 km, and in the along-track direction after synthetic-aperture processing is 0.3 to 1 km. The transmitted signal is a 10-W, 85-μs chirped (linearly frequency-modulated) pulse emitted from a 10-m-long dipole antenna. After downlink to Earth, coherent azimuth sums on ~1500 pulses taken at a pulse repetition frequency of 700 Hz result in a signal-to-noise ratio of 30 to 40 dB for a relatively smooth surface (*17*, *18*). Waves that are transmitted into the subsurface reflect from dielectric discontinuities and return to the instrument at greater time delay than the nadir surface echo. The primary obstacle to the identification of subsurface echoes is interference from off-nadir surface echoes (known as "surface clutter") that arrives at the radar receiver with the same time delay as that of subsurface echoes. The data described here were acquired in January and February 2007, on orbits 2202, 2413, 2624, and 2835. The ground tracks of the radar are located within Planum Australe's Promethei Lingula region (Fig. 1). Here we report on the SPLD stratigraphy as mapped by SHARAD in Promethei Lingula and interpret this information in terms of the depositional and erosional history.

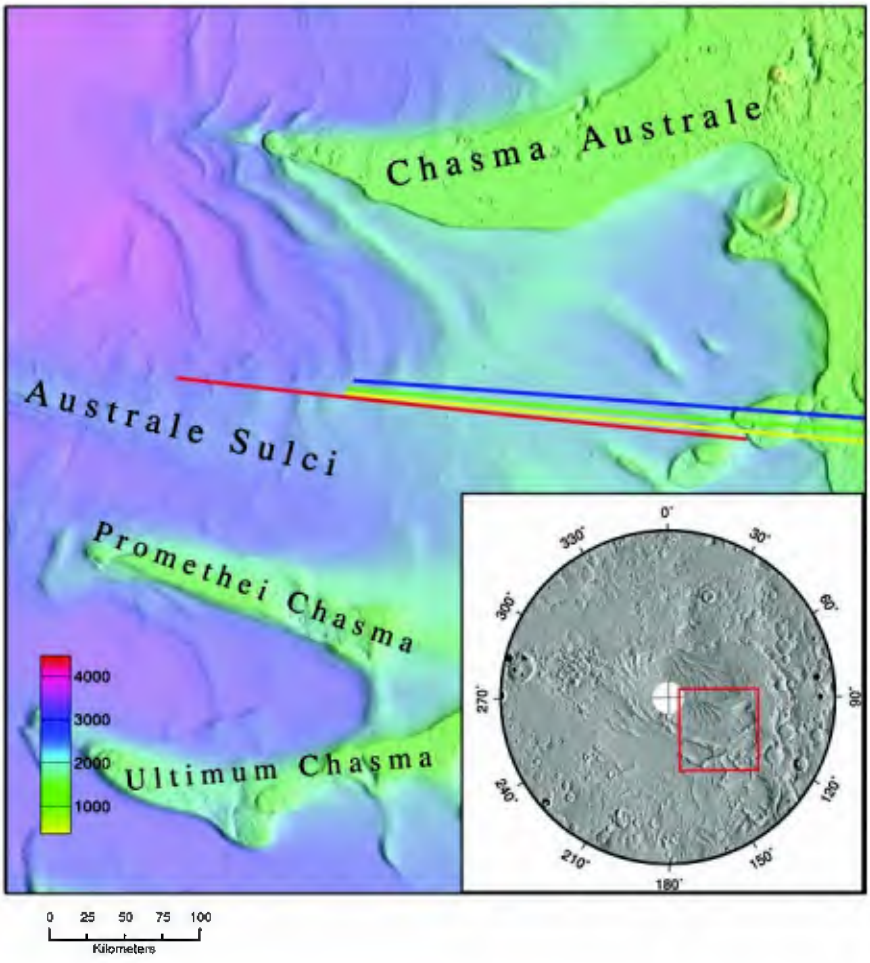

Fig. 1. Topography of the Promethei Lingula region. Promethei Lingula is the extension of the Planum Australe plateau delimited by Chasma Australe to the top, Ultimum Chasma to the bottom, and Promethei Planum to the right. The ground tracks of the MRO spacecraft during SHARAD data acquisitions are shown in red for orbit 2202, in yellow for orbit 2413, in green for orbit 2624, and in blue for orbit 2835. The inset shows the location in the south polar area of Mars.

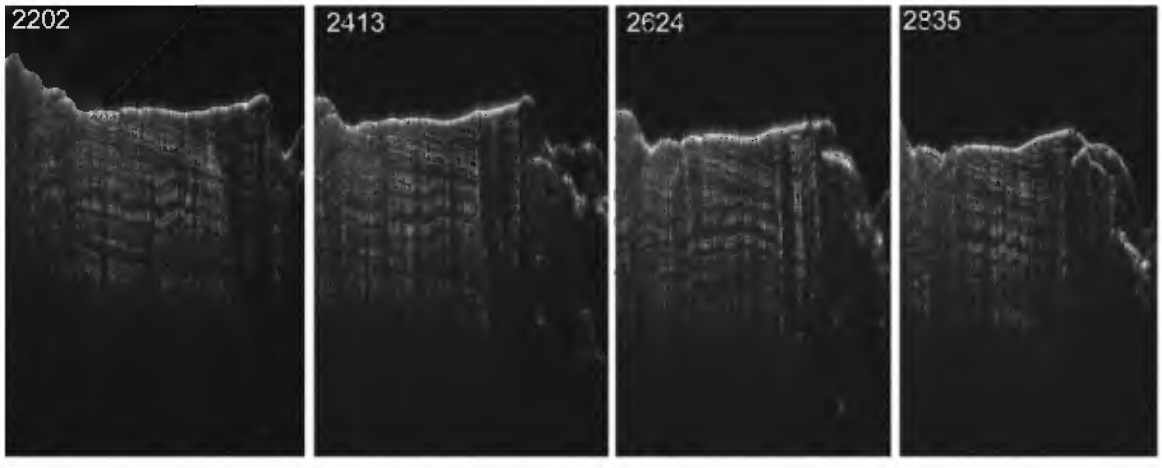

Fig. 2. Radargrams for orbits 2202, 2413, 2624, and 2835. A radargram is a two-dimensional cross section of the surface and subsurface in which brightness corresponds to echo power. The vertical axis is the two-way pulse travel time, and the horizontal axis is the distance of the spacecraft along its ground track. Similar subsurface layering structure is seen in these four closely spaced, parallel tracks.

Roughly half of Promethei Lingula is dissected by canyon systems. These include deep canyons radial to the Promethei Lingula distal margin (chasmata) and smaller, curvilinear canyons perpendicular to the chasmata commonly referred to as "spiral troughs" (Fig. 1). The origin of the chasmata has been attributed to dissection by katabatic wind (*12*, *19*, *20*) or to basal melting (*21*), whereas development of curvilinear canyons has been attributed to aeolian erosion (*20*, *22*) or to ductile deformation (*23*) of the SPLD.

SHARAD data were acquired during four closely spaced (<5 km), nearly parallel orbit segments (Fig. 1). These data (Fig. 2) are all characterized by a multilayered internal structure with dozens of internal reflections. Many of these reflections are traceable over distances of up to 150 km over the smooth area extending from the outer edge to the central part of the Planum Australe plateau (from right to left in Fig. 2). There are several bands (packets) containing many thin reflectors running parallel or subparallel to the surface, separated by thicker dark bands. To determine if they arise from subsurface interfaces or come from surface topographic features at the same time delay, we ran a high-fidelity model of the expected contribution of off-nadir topographic clutter using Mars Orbiter Laser Altimeter (MOLA) data (*7*, *24*, *25*). Results show no visible surface topographic feature that explains the observed bands; hence, we conclude that they are subsurface reflectors. This banded structure is similar, and certainly related, to the layering visible in optical images, and radar reflections are likely caused by intralayer compositional variations in dust content or density. Sets of reflectors can be correlated among the four radargrams, giving us confidence that the same layered structure extends laterally (across track) for several kilometers. Reflections are seen down to depths of about 1 km, consistent with the very low attenuation through the SPLD observed by MARSIS. However, such reflections are at a shallower depth than the deepest reflection in the MARSIS radargrams over the same area, which are found at 1.3 km and correspond to the local plateau height relative to the surrounding plains (*6*). We deem that the lack of any deeper reflectors is more likely due to attenuation or scattering of the SHARAD radar signal than to the character of the plateau basal interface.

The distinct subsurface layered structure noted above is not present along the entire length of the four SHARAD ground tracks. In some areas, these dielectric interfaces pinch out or disappear entirely. Possible reasons for these changes in the echo behavior include (i) tilting of the layers, which can move the specular reflection from a smooth interface out of the Doppler bandwidth of the processed data; (ii) increased surface roughness that decreases the effective amount of radar signal transmitted into the subsurface; or (iii) changes in the geologic structure or physical state of the materials that diminishes their dielectric contrast.

From analysis of the radargrams, it is possible to identify four main boundaries (colored lines in Fig. 3) that separate different dielectric sequences. The first sequence, limited at the base by the yellow boundary and located in time between 1.7 and 5.3 μs of depth below the surface, is dipping toward the right. Several of the upper layers in this sequence terminate at the surface, which is nearly horizontal in this segment. Below this reflector a second one (in white) is detectable at a time depth of about 4.3 to 5.6 μs. Beneath such an interface a second well-defined sequence of layers is clearly visible up to a time depth of about 5.6 to 7.1 μs where the third main reflector (in orange) closes the series. Finally, below it another multilayered structure, limited by a reflector (in light blue) located at a depth of about 11.0 to 12.9 μs, is also visible.

To convert echo time delays to depths requires assumptions about the material that the radar pulse is passing through. As mentioned above, the SPLD may consist mostly of water ice (*6*). We thus convert time to depth by assuming a real part of the relative permittivity of 3.5, corresponding to that of water ice with a few percent of dust. The four reflectors shown in Fig. 3 are located, from top to bottom, at depths of about 130 to 420 m, 340 to 450 m, 450 to 570 m, and 890 to 1030 m. Because the depths scale by the inverse of the square root of the dielectric constant, small variations in material (i.e., dust content) will not have a profound effect on calculated depths.

Above the first reflector in Fig. 3, the layers are continuous and generally of even thickness laterally. Below the second reflector the same observation applies. Between the two, the layer sequence goes from thick (about 240 m) to nearly zero. The layers become difficult to follow within this wedge-shaped region. We propose two possible interpretations for this morphology: (i) The pinching out of the layers in the wedge-shaped region is an erosional feature (an unconformity); or (ii) the shape of this region is a primary feature of the deposition, i.e., the thickness of some layers varies laterally. The first interpretation is consistent with conclusions from a study of exposed layers in Promethei and Ultimum Chasmata (Fig. 1) (*19*). However, because there is no clear image of truncation of the bedding along a dipping boundary in the wedge-shaped region, we are unable to rule out interpretation (ii).

We interpret the dipping layers that are truncated at the surface within Australe Sulci as due to erosion of the plateau surface rather than due to lateral variations in SPLD accumulation rate, because this last process would be unable to produce the observed constant thickness of the layers. This interpretation is consistent with the observation of erosional surface features in Australe Sulci, whose shape and direction may be controlled by the wind, most likely by off-pole katabatic winds (*12*). The local stratigraphic evolution can thus be interpreted as consisting of at least four stages: (i) essentially uniform deposition of a lower package; (ii) erosion at an angle, or laterally variable deposition; (iii) renewed deposition on the angled surface; and (iv) truncation of

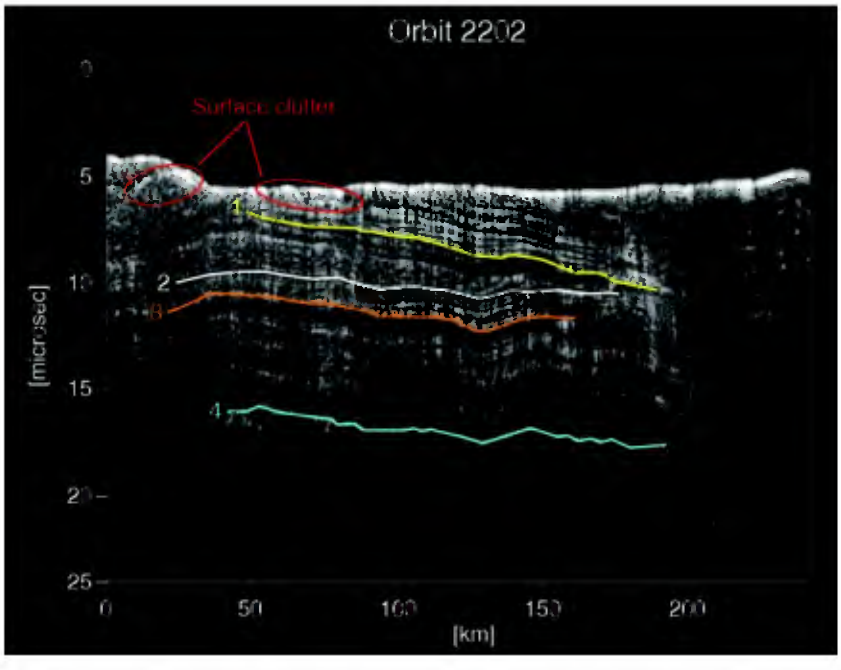

Fig. 3. Enlarged view of data for orbit 2202. Four main reflectors, which separate different dielectric sequences, are marked with lines of yellow, white, orange, and light blue. Red ellipses highlight echo features identified as surface clutter through radar surface echo simulation (see text).

the angled package to the present horizontal surface as result of erosion.

Despite the age uncertainties of the polar deposits, the strength of CO_2 ice is insufficient to support the long-term topography of the polar caps (*26*). SHARAD data are consistent with a mechanically strong plateau material, as we see no evidence, such as folding or faulting, for flow in the bulk of the plateau's layered structure. However, flow resulting in broad-scale changes in layer thickness or flow at the very base of the deposits cannot be ruled out by these observations. The continuity of layers, spanning distances of up to 150 km, is evidence that the depositional processes that formed Planum Australe were regional in scale, as already inferred from layer correlation studies of exposures in Australe Mensa (*27*) and Promethei Lingula (*19*). Spectral and albedo observations of the surface indicate that the plateau surface is covered by an optically thick layer of dust or rocky material (*7*), but we do not see evidence in our data that can be interpreted in terms of an ice-free surface layer, perhaps because of its small thickness compared to SHARAD vertical resolution.

References and Notes

1. J. R. Petit *et al.*, *Nature* **399**, 429 (1999).
2. K. L. Tanaka, E. J. Kolb, *Icarus* **154**, 3 (2001).
3. D. E. Smith *et al.*, *Science* **284**, 1495 (1999).
4. S. Byrne, A. P. Ingersoll, *Science* **299**, 1051 (2003).
5. J.-P. Bibring *et al.*, *Nature* **428**, 627 (2004).
6. J. J. Plaut *et al.*, *Science* **316**, 92 (2007).
7. S. Douté *et al.*, *Planet. Space Sci.* **55**, 113 (2007).
8. O. B. Toon, J. B. Pollack, W. Ward, J. A. Burns, K. Bilski, *Icarus* **44**, 552 (1980).
9. P. Thomas, S. Squyres, K. Herkenhoff, A. Howard, B. C. Murray, in *Mars*, H. H. Kieffer, B. M. Jakosky, C. W. Snyder, M. S. Matthews, Eds. (Univ. of Arizona Press, Tucson, 1992), pp. 767–795.
10. M. T. Mellon, *Icarus* **124**, 268 (1996).
11. K. E. Herkenhoff, J. J. Plaut, *Icarus* **144**, 243 (2000).
12. M. R. Koutnik, S. Byrne, B. C. Murray, A. D. Toigo, Z. A. Crawford, *Icarus* **174**, 490 (2005).
13. G. Picardi *et al.*, *Science* **310**, 1925 (2005).
14. D. C. Nunes, R. J. Phillips, *J. Geophys. Res.* **111**, E06S21 (2006).
15. M. C. Malin, K. S. Edgett, *J. Geophys. Res.* **106**, 23429 (2001).
16. J. E. Graf *et al.*, *Acta Astronaut.* **57**, 566 (2005).
17. R. Seu *et al.*, *J. Geophys. Res.* **112**, E05S05 (2007).
18. R. Seu *et al.*, *Planet. Space Sci.* **52**, 157 (2004).
19. E. J. Kolb, K. L. Tanaka, *Mars* **2**, 1 (2006).
20. A. D. Howard, *Icarus* **144**, 267 (2000).
21. S. M. Clifford, *J. Geophys. Res.* **92**, 9135 (1987).
22. A. D. Howard, *Icarus* **34**, 581 (1978).
23. D. A. Fisher, *Icarus* **105**, 501 (1993).
24. J.-F. Nouvel, A. Herique, W. Kofman, A. Safaeinili, *Radio Sci.* **39**, RS1013 (2004).
25. MOLA topographic data at 1/128 degree per pixel grid spacing were used to simulate echoes from the cross-track region for each SHARAD subsurface sounding observation. Along-track sources were suppressed because SHARAD data processing achieves this by aperture synthesis.
26. J. F. Nye, W. B. Durham, P. M. Schenk, J. M. Moore, *Icarus* **144**, 449 (2000).
27. S. Byrne, A. B. Ivanov, *J. Geophys. Res.* **109**, E11001 (2004).

28. The Shallow Subsurface Radar (SHARAD) was provided by the Italian Space Agency, and its operations are led by the INFOCOM Department, University of Rome "La Sapienza." Thales Alenia Space Italia is the prime contractor for SHARAD and is in charge of in-flight instrument commissioning and of the SHARAD Operations Center. The Mars Reconnaissance Orbiter mission is managed by the Jet Propulsion Laboratory, California Institute of Technology, for the NASA Science Mission Directorate, Washington, DC. Lockheed Martin Space Systems, Denver, is the prime contractor for the orbiter.

23 April 2007; accepted 16 August 2007
10.1126/science.1144120

REPORT

Density of Mars' South Polar Layered Deposits

Maria T. Zuber,[1]* Roger J. Phillips,[2] Jeffrey C. Andrews-Hanna,[1] Sami W. Asmar,[3] Alexander S. Konopliv,[3] Frank G. Lemoine,[4] Jeffrey J. Plaut,[3] David E. Smith,[4] Suzanne E. Smrekar[3]

Both poles of Mars are hidden beneath caps of layered ice. We calculated the density of the south polar layered deposits by combining the gravity field obtained from initial results of radio tracking of the Mars Reconnaissance Orbiter with existing surface topography from the Mars Orbiter Laser Altimeter on the Mars Global Surveyor spacecraft and basal topography from the Mars Advanced Radar for Subsurface and Ionospheric Sounding on the Mars Express spacecraft. The results indicate a best-fit density of 1220 kilograms per cubic meter, which is consistent with water ice that has ~15% admixed dust. The results demonstrate that the deposits are probably composed of relatively clean water ice and also refine the martian surface-water inventory.

The martian south polar layered deposits (SPLD) (Fig. 1) contain the south polar residual ice cap and smooth, low-albedo surroundings that collectively rise ~3 km above the surrounding cratered highlands terrain (*1*). The residual polar-cap component is believed to be composed of water ice with an unknown admixed dust component that is overlain by a thin (1- to 10-m) predominantly CO_2 cover (*2*–*4*). The CO_2 veneer contains "swiss cheese–like" shallow depressions (*5*) that reveal the underlying water ice at their bases. The more spatially extensive part of the SPLD (Fig. 1) has a low albedo and a dustlike spectral signature, which raises the question of whether the dominant component of the SPLD as a whole is volatile (H_2O and/or CO_2) or dust. This question is relevant to establishing an accurate inventory of surface volatiles on Mars.

In this study, we used initial high-resolution gravity observations from X-band (8.4 GHz) Doppler tracking of the Mars Reconnaissance Orbiter (MRO) (*6*) together with the volume obtained by combining surface topography from the Mars Orbiter Laser Altimeter (MOLA) (*7*) and basal topography from the Mars Advanced Radar for Subsurface and Ionospheric Sounding (MARSIS) (*8*) to calculate the density of the SPLD and constrain their composition. The MRO's orbital periapsis altitude of ~255 km above the south pole of Mars provides considerably higher spatial resolution measurements (140-km block size) than did previous Mars missions (*9*) and permits the gravitational attraction of the SPLD and underlying crust to be resolved sufficiently for regional modeling for the first time (Fig. 2).

We found the best-fit density by calculating the predicted gravity field from the observed structures of the SPLD and of the crust and mantle. The key unknowns were the densities of the crust, mantle, and SPLD and the topography along the crust/mantle interface (the Moho). The densities of the martian crust and mantle were taken to be 2900 and 3500 kg m^{-3}, respectively (*10*). Because it is not possible to solve simultaneously for both the SPLD density and the Moho topography, we represented the Moho beneath the SPLD by assuming that the topography before loading by the SPLD is in a state of partial isostatic compensation. The best-fit degree of compensation outside the SPLD of 91% was applied to the crustal topography beneath the SPLD to estimate the depth to the Moho. The lack of observed flexure in MARSIS profiles (*8*) suggests support by a thick lithosphere (*11*). We calculated the deflection of the Moho by the

[1]Department of Earth, Atmospheric and Planetary Sciences, Massachusetts Institute of Technology, 77 Massachusetts Avenue, Cambridge, MA 02139–4307, USA. [2]Department of Earth and Planetary Sciences, Washington University, St. Louis, MO 63130, USA. [3]Jet Propulsion Laboratory, California Institute of Technology, 4800 Oak Grove Drive, Pasadena, CA 91009–8099, USA. [4]Solar System Exploration Division, NASA Goddard Space Flight Center, Greenbelt, MD 20771, USA.

*To whom correspondence should be addressed. E-mail: zuber@mit.edu